

Confronting Dark Matter Capture Rate with Continuous Gravitational Wave Probe of Local Neutron Stars

Pooja Bhattacharjee^{1,*} and Amit Dutta Banik^{2,†}

¹*LAPP, CNRS, USMB, F-74940 Annecy, France*

²*Physics and Applied Mathematics Unit, Indian Statistical Institute, Kolkata-700108, India*

Continuous gravitational waves (CGWs) from various astrophysical sources are one of the many future probes of upcoming Gravitational Wave (GW) search missions. Neutron stars (NSs) with deformity are one of the leading sources of CGW emissions. In this work, for the first time, a novel attempt to estimate the dark matter (DM) capture rate is performed using CGW as the probe to the local NS population. Competitive bounds on DM capture from the local NS population are reported when compared with DM direct search experiments and other astrophysical observations.

arXiv:2404.15038v2 [astro-ph.HE] 14 May 2024

* pooja.bhattacharjee@lapp.in2p3.fr

† amitdbanik@gmail.com

I. INTRODUCTION

It is nearly half a century ago, that the existence of dark matter (DM) has been confirmed from the observations of spiral galaxies. Later experiments like Planck [1] also verified the presence of DM in the Universe with the observation of cosmic microwave background radiation. However, the nature of DM remains an enigma to be resolved as the particle physics of the Standard Model (SM) fails to provide a viable DM candidate. Despite its prevalence, the fundamental nature of DM remains unknown, fueling intense research efforts to detect and understand its properties. Among various DM searches, indirect detection of DM [2] has gained a lot of attention as the terrestrial direct detection experiments failed to detect any promising DM-nucleon scattering event. Indirect detection methods involve searching for the products resulting from annihilation or decay of DM particles (χ), such as gamma rays, neutrinos, or cosmic rays, which can provide indirect evidence of its presence [3]. This detection method has the potential to contribute to the ongoing quest to unravel the enigma of DM and shed light on the fundamental nature of the universe's underlying structure.

Neutron stars (NSs), the most compact stars in the Universe, emerge from the core-collapse supernova explosions of massive stars [4]. Their intense gravitational pull and diminutive size render them potent traps for passing DM particles, potentially accumulating them over time [5]. Despite being smaller than brown dwarfs (BDs) [6–8], white dwarfs (WDs) [9, 10], and stars [11, 12], NSs possess a superior advantage for DM capture owing to their substantial gravitational pull and efficient interaction rate with DM [9, 13, 14]. Their core, primarily composed of tightly packed neutrons, fosters conditions conducive to DM interactions [15, 16]. Moreover, the absence of electromagnetic interference facilitates uninterrupted capture processes, augmenting the efficiency of DM accumulation [4]. This advantage over BDs and stars positions NSs as promising candidates for indirect DM search [4]. The accumulation of DM within NSs yields a spectrum of potentially observable outcomes, including detection through the annihilation via long-lived mediator (ϕ) into neutrinos, gamma rays, or other SM particles that escape the surface of NSs [17–20]. The DM capture rate in Sun, WDs, BDs, and Galactic NS has been explored in several studies [8, 9, 14, 19, 21–30].

Additionally, DM capture in NSs may induce significant consequences such as kinetic heating [31], collapsing into black holes [32], alteration of NS merger rates [13], or modification of gravitational wave signatures from binary NS mergers [33]. They are also considered as one of the smoking gun signatures of continuous gravitational waves (CGW) [34, 35]. The rotation of NSs causes them to deform, generating a quadrupole moment that serves as the source of continuous GW emanating from the NS itself [36, 37]. Recent studies have pursued the null detection of continuous gravitational waves to impose constraints on their population [38], providing an estimation of the local population of NSs near Earth.

In this study, we undertake a comprehensive multi-wavelength approach, expanding our inquiry from gamma rays to neutrinos in the pursuit of detecting DM particles confined within NSs. This study aims to scrutinize the DM capture rate, particularly within nearby NSs located approximately 0.6 kpc from Earth, by probing the DM annihilation via long-lived mediator (ϕ) with space-based or ground-based telescopes. The local NS population inferred from CGW emissions allows us to particularly investigate the cumulative population from around $\sim 10^5$ local NSs within 0.6 kpc [38]. Neutrino and gamma-ray searches offer unique advantages in the quest for DM. Both gamma rays and Neutrinos, being electrically neutral, travel directly from the source location unhindered by the Galactic or extra-galactic magnetic field. Neutrino signals, due to their weak interaction, travel unhindered from their sources without deflection or attenuation and can gain insights into dense sources, even those at cosmological distances, which other SM particles cannot reach. Telescopes like Fermi-LAT [39, 40], LHAASO [41, 42], CTA [43, 44], SWGO [42], etc. search for sources of gamma rays from various celestial objects whereas IceCube [45], IceCube-Gen2 [46], TRIDENT [47], KM3NET [48] experiments search for neutrino events from similar astrophysical bodies.

The paper is organized as follows. In Sec. II, we canvass the details of a few local NSs of our interest and nearby NS populations obtained from the CGW searches as primary sources of observation. In Sec. III, we brief on the theoretical framework of DM capture and annihilation within NS with long-lived mediators followed by a discussion on present and future experiments of significance to our analysis in Sec. IV. The bounds on DM scattering cross-sections obtained from the analysis with detector sensitivity for local NSs along with the NS population estimate of CGW searches are presented in Sec. V. We summarise the work with concluding remarks in Sec. VI.

II. SOURCE SELECTION

A. Observed nearby NSs

For this work, we consider the local NSs that lie within 0.6 kpc [49] from Earth. We chose some nearby NSs from ref. [49]. We follow a few conditions to select our candidates:

- Distance: There are nearby i.e. within 0.6 kpc from Earth.
- Age: Old ($> \text{Myr}$) so that DM annihilation rate and capture rate can reach equilibrium.

TABLE I. Source Details: Column I: Name of our selected NS; Column II & III: R.A. and DEC; Column IV: Distance to the local NSs; Column V: Mass in M_{\odot} ; Column VI: Radius (R_{NS}) in km; Column VII: Age. We take the parameters of Column I-IV from ref. [49]. For mass and radius, we consider the general expected values for NS. For age estimation, we rely on the ATNF catalog [50].

Common (ID)	Name	RA (deg)	DEC (deg)	Distance (kpc)	Mass (M_{\odot})	Radius (km)	Estimated age (yr)
J0711-6830 (Source 1)		107.9758	-68.5132	0.11	1.4	10-15	5.84e9
J0745-5353 (Source 2)		116.2596	-53.8561	0.57	1.4	10-15	1.25e6
J0945-4833 (Source 3)		146.4094	-48.5540	0.35	1.4	10-15	1.09e6
J0957-5432 (Source 4)		149.4834	-54.5344	0.45	1.4	10-15	1.66e6
J1000-5149 (Source 5)		150.1173	-51.8328	0.13	1.4	10-15	4.22e6
J1017-7156 (Source 6)		154.4639	-71.9449	0.26	1.4	10-15	1.43e10
J1725-0732 (Source 7)		261.3012	-7.5498	0.20	1.4	10-15	8.85e6
J1755-0903 (Source 8)		268.7932	-9.0643	0.23	1.4	10-15	3.9e6

B. Local NS population predicted from CGW

In this section, we delve into the anticipated count of nearby NSs by exploring CGWs. The emission of gravitational waves from a rotating neutron star is contingent upon asymmetric deformations within its structure, manifesting as the star's ellipticity (ϵ) [36, 37]. With an estimated age for the Milky Way of approximately 10^{10} years and a Galactic supernovae rate of 1 per century [51], it's plausible that around $N_0 \sim 10^8$ NSs have been generated within our Galaxy to date. However, only a fraction of these, primarily a few thousand, have been identified through electromagnetic searches, largely comprising radio pulsars [52]. The detection of gravitational waves may facilitate the discovery of some of the remaining unidentified NSs and enable the investigation of their morphological distribution [34, 35]. A recent investigation by ref. [38], conducted an extensive search for CGWs originating from unidentified Galactic NSs to establish constraints on their shapes. This study employed a straightforward model of the spatial and spin distributions of Galactic NSs to estimate the total count of NSs (N_{ns}) within proximity to Earth, given a specific upper limit on ϵ .

As detailed in Sec. II A, our focus is solely on the local NSs within 0.6 kpc from Earth. Following the population model proposed by ref. [38], the estimated number of NSs within a distance 0.6 kpc from Earth with $\epsilon \sim 10^{-5}$ is found to be $N_{\text{ns}} \simeq 10^5$. In subsequent sections, we elaborate on how such a large expected N_{ns} population within 0.6 kpc of Earth can impact our investigation.

III. FORMULATION

This section elucidates the key factors influencing the anticipated gamma-ray and neutrino flux stemming from DM captured within NSs. Our focus is on scenarios where DM interacts with nucleons, resulting in gravitational binding to

the NS and subsequent accumulation within it. This occurs when, following single or multiple scatterings, the velocity of the DM particle diminishes below the NS escape velocity, thus preventing evaporation.

The computation can be segmented into three primary parts:

- A) DM capture into NSs, contingent upon the local density and velocity distribution of DM, alongside the scattering cross-section of DM particles with neutrons.
- B) The annihilation rate of DM particles ensnared gravitationally within NSs.
- C) The emission of gamma-rays and neutrinos ensuing from the decay of long-lived mediators generated through DM annihilation.

A. DM capture rate inside NSs

The ‘‘maximum capture rate’’ (C_{\max}) delineates the scenario where DM particles traversing through NSs become captured. An initial evaluation for C_{\max} in a DM environment, characterized by parameters such as radius R_{NS} , DM number density $n_\chi = \rho_\chi/m_\chi$, velocity dispersion (\bar{v}), and relative velocity (v_0), is given by Eq. 1. The escape velocity (v_{esc}) is dictated by the mass M_{NS} and radius R_{NS} of the NS [21].

$$C_{\max}(r) = \pi R_{\text{NS}}^2 n_\chi(r) v_0 \left(1 + \frac{3}{2} \frac{v_{\text{esc}}^2}{\bar{v}(r)^2} \right) \quad (1)$$

Here, $v_0 = \sqrt{8/(3\pi)}\bar{v}$, and $\bar{v}(r) = 3/2v_c(r)$, where $v_c(r) = \sqrt{GM(r)/r}$ represents the circular velocity at any galactocentric distance r , with G denoting the gravitational constant and $M(r)$ indicating the total Galactic mass encompassed within r . Regarding the DM density distribution, we adopt the Navarro-Frenk-White (NFW) density profile [53] with $\rho_\chi(r=R_\odot) \equiv \rho_0 = 0.39 \text{ GeV cm}^{-3}$ [54].

In a realistic setting, the perturbative approach must be accounted for, as not all DM particles passing through are captured. As mentioned, DM particles can undergo multiple scatterings, and when their velocity falls below the escape velocity of the NS, they become captured. The probability of experiencing N scatterings before being trapped inside the NS is defined by Eq. 2, where $\tau = \frac{3}{2} \frac{\sigma_{\chi n}}{\sigma_{\text{sat}}}$, with $\sigma_{\chi n}$ denoting the DM-nucleon scattering cross-section, $\sigma_{\text{sat}} = \pi R_{\text{NS}}^2/N_n$ representing the saturation cross-section, and $N_n = M_{\text{NS}}/m_n$ indicating the number of nucleons in the target. The total capture rate (C_{tot}) encompasses both single and multiple scatterings, as delineated in Eq. 3.

$$p_N(\tau) = 2, \int_0^1 dy, \frac{y, e^{-y\tau}, (y\tau)^N}{N!} \quad (2)$$

$$C_{\text{tot}}(r) = \sum_{N=1}^{\infty} C_N(r) \quad (3)$$

The capture rate corresponding to N scatterings, C_N , is delineated by Eq. 4 [5, 55]. Here, v_N is defined as $v_N = v_{\text{esc}}(1 - \beta_+/2)^{-N/2}$, where $\beta_+ = 4m_\chi m_n/(m_\chi + m_n)^2$. For a large number of scatterings ($N \gg 1$), $(v_N^2 - v_{\text{esc}}^2)$ predominates over \bar{v}^2 , and C_N approximates $\approx p_N C_{\max}$.

$$C_N(r) = \frac{\pi R_{\text{NS}}^2 p_N(\tau)}{1 - 2GM_{\text{NS}}/R_{\text{NS}}} \frac{\sqrt{6}n_\chi(r)}{3\sqrt{\pi}\bar{v}(r)} \left[(2\bar{v}(r)^2 + 3v_{\text{esc}}^2) - (2\bar{v}(r)^2 + 3v_N^2) \exp\left(-\frac{3(v_N^2 - v_{\text{esc}}^2)}{2\bar{v}(r)^2}\right) \right] \quad (4)$$

B. DM annihilation to gamma rays and neutrinos

Ignoring the impact of evaporation (which is $\sim \text{MeV}$ [56]), the total number of DM particles, represented as $N(t)$, accumulated within the core of the NS at time t , is governed by the DM number abundance in Eq. 5:

$$\frac{dN(t)}{dt} = C - C_{\text{ann}} N^2(t), \quad (5)$$

In this context, $C = \min[C_{\text{tot}}, C_{\text{max}}]$ denotes the total capture rate under the condition that the perturbative estimation is deemed valid, while C_{ann} signifies the annihilation rate defined as $C_{\text{ann}} = \frac{\langle \sigma v \rangle}{V_{\text{NS}}}$; where $\langle \sigma v \rangle$ represents the annihilation cross-section for thermal DM and V_{NS} denotes the volume within the NS where annihilation occurs. If we disregard the influence of evaporation, the solution to Eq. 5 can be expressed as:

$$N(t) = C t_{\text{eq}} \tanh \frac{t}{t_{\text{eq}}} \quad (6)$$

The equilibrium time, $t_{\text{eq}} \equiv \frac{1}{\sqrt{C_{\text{ann}} C}}$, represents the time required to reach equilibrium between DM capture rate and annihilation rate in the absence of evaporation. If equilibrium is achieved today (i.e. $t_{\text{NS}} \geq t_{\text{eq}}$), the total annihilation rate (Γ_{ann}) is solely dependent on the DM capture rate, i.e. $\Gamma_{\text{ann}} \rightarrow \frac{C}{2}$.

C. Gamma-ray and neutrino spectrum: For DM annihilation via long-lived mediators

In this investigation, we delve into the emission of gamma rays and neutrinos resulting from the annihilation of DM. Typically, when DM particles undergo direct annihilation into quark-anti-quark pairs, they expect to generate detectable signals in the form of gamma rays and neutrinos as the final state products. However, when examining DM annihilation within celestial bodies such as NSs, there exists a possibility that if DM particles directly annihilate into SM final states, they could become confined within the NS, thereby inducing its heating. This heating phenomenon could potentially be observed using the James Webb Space Telescope (JWST), as recently discussed in reference [8], although such observations pose significant challenges due to current instrumental limitations. Nevertheless, the chances of detecting a signal are enhanced when DM annihilation to SM states occurs via long-lived mediators (ϕ) that can escape the NS's surface, as proposed in various references [17, 18, 57–68]. The decay products of these mediators may potentially yield observable signals in gamma-ray or neutrino telescopes.

Nonetheless, there remains a possibility that these mediators might interact with SM constituents within the NS before escaping, potentially resulting in a significant decrease in the observed flux of gamma rays and neutrinos. As illustrated in [8, 22], it is possible to substantially mitigate this attenuation by carefully selecting appropriate model parameters. Hence, for the sake of simplicity and for ease of comparison with existing literature, we focus on the scenario where the long-lived mediator facilitates DM annihilation outside the NSs, such as $\chi\chi \rightarrow \phi\phi \rightarrow 4\gamma$ and $\chi\chi \rightarrow \phi\phi \rightarrow \nu\bar{\nu}\nu\bar{\nu}$. Additionally, we make the assumption that $m_\phi \ll m_\chi$, under which the provided formulas remain applicable even though this approximation removes the dependence on the additional parameter m_ϕ .

The Eqs. 7 and 8 describe the differential flux of gamma rays and neutrinos reaching Earth as a result of DM annihilation via a long-lived mediator.

$$\frac{d\phi_\gamma}{dE_\gamma} = \frac{\Gamma_{\text{ann}}}{4\pi d_{\text{NS}}^2} \times \left(\frac{dN_\gamma}{dE_\gamma} \right) \times P_{\text{surv}}, \quad (7)$$

$$\frac{d\phi_\nu}{dE_\nu} = \frac{\Gamma_{\text{ann}}}{4\pi d_{\text{NS}}^2} \times \left(\frac{1}{3} \frac{dN_\nu}{dE_\nu} \right) \times P_{\text{surv}}, \quad (8)$$

In this context, d_{NS} denotes the distance between Earth and the location of our selected NSs in sec. II A. It also takes into account the contribution of the ‘‘survival probability’’ (P_{surv}) for gamma rays and neutrinos reaching the detectors, which is nearly unity within the range of mediator decay lengths. Within the neutrino flux expression, there is a factor of $\frac{1}{3}$ to incorporate all neutrino flavors. In our scenarios, we are considering neutrinos arriving from distances of a few kpc, allowing us to confidently neglect the neutrino oscillation effects and proceed with the assumption that the proportion of neutrino flavors reaching Earth follows a ratio of $\nu_e : \nu_\mu : \nu_\tau = 1 : 1 : 1$.

Under our stated hypothesis, where $m_\phi \ll m_\chi$, the reliance on m_ϕ is removed, leading to the conceptualization of the neutrino and gamma-ray spectrum as a box-shaped distribution, as described by ref. [69] in Eq. 9.

$$\frac{dN_{\gamma,\nu}}{dE_{\gamma,\nu}} = \frac{4\Theta(E - E_-)\Theta(E_+ - E)}{\Delta E}, \quad (9)$$

Here, Θ signifies the Heaviside-theta function. The energy bounds are denoted by $E_{\pm} = (m_{\chi} \pm \sqrt{m_{\chi}^2 - m_{\phi}^2})/2$, with the width of the box function defined as $\Delta E = \sqrt{m_{\chi}^2 - m_{\phi}^2}$.

IV. CURRENT AND FUTURE GENERATION TELESCOPES

Studying the indirect detection of DM signals through multiwavelength observations, particularly in gamma-ray and neutrino wavelengths, offers a promising avenue to unravel the mysteries of DM. Gamma rays and neutrinos are two fundamental messengers that can provide complementary insights into the elusive nature of DM particles. Gamma rays, emitted from astrophysical sources or produced by DM annihilation or decay, can unveil signatures indicative of DM interactions. On the other hand, neutrinos, being weakly interacting particles, can traverse vast cosmic distances without being absorbed or deflected, offering a pristine view of the Universe's most distant and obscured regions.

Combining data from gamma-ray and neutrino observations enables us to construct a comprehensive picture of DM distribution and behavior across different cosmic scales. Moreover, cross-correlating these observations with other astronomical datasets, such as those from gravitational wave detectors and galaxy surveys, enriches our understanding of DM's role in shaping the cosmos. Multiwavelength studies thus stand as a powerful strategy to decipher the enigmatic properties of DM and elucidate its profound impact on the Universe.

In sec. III C, we discuss the DM annihilation spectra through long-lived mediators. In this section, we probe the expected gamma-ray and neutrino flux resulting from DM captured inside NS with the current and future generations of neutrino and gamma-ray telescopes.

A. With current and future neutrino telescopes

Neutrino telescopes offer a novel avenue for probing DM [26, 70] by detecting neutrinos. These telescopes complement traditional detection methods, providing insights into DM distribution and properties through neutrino emissions from potential DM sources across the Universe.

IceCube, a massive cubic-kilometer neutrino detector situated at the South Pole, was completed in 2010. Originally proposed based on theoretical calculations in 1998, it was envisioned to be sensitive enough to detect high-energy neutrinos from phenomena such as AGN jets or GRBs [71]. As the first experiment of its kind, IceCube has achieved significant milestones, including the discovery of a diffuse extraterrestrial neutrino flux in 2013 [72] and the detection of neutrino emission from a flaring blazar in 2017 [73, 74]. Despite dedicated efforts to identify the sources of cosmic neutrinos through various analyses, such as all-sky survey [45], transient [75–77], and AGN catalog stacking searches [78, 79], conclusive results remain elusive. This suggests the possibility of multiple weaker sources contributing to the diffuse flux [80], such as starburst galaxies [81], which would necessitate improved pointing resolution for resolution [82].

IceCube-Gen2, an extension of the IceCube Neutrino Observatory in Antarctica, aims to explore the high-energy neutrino sky from TeV to PeV energies [83, 84]. It promises five times better sensitivity for neutrino sources compared to the current IceCube detector. With 120 new strings and larger spacing between them, IceCube-Gen2 will enhance sensitivity for neutrinos above 10 TeV and target detection of neutrinos exceeding 100 PeV [84]. The ongoing IceCube upgrade will improve detection thresholds down to 1 GeV, enhancing capabilities for various physics studies [46]. IceCube-Gen2's larger instrumented area will enable the detection of fainter neutrino sources, positioning it as the world's leading neutrino observatory. It holds promise for diverse scientific inquiries, including DM searches, particle physics studies, and the detection of supernova neutrinos [85].

TRIDENT, a next-generation neutrino telescope slated for construction in the South China Sea [47], is poised to transform our understanding of high-energy astrophysical neutrinos. Its primary goal is to detect multiple sources and enhance measurements of cosmic neutrino events across all flavors. With improved angular resolution and sensitivity

[86], TRIDENT aims to pinpoint sources within the diffuse flux identified by IceCube [47]. Positioned near the equator, TRIDENT will provide extensive visibility of the neutrino sky due to Earth's rotation, bolstering the global network of neutrino observatories [47]. Furthermore, the reduced light scattering in water compared to IceCube's glacial ice promises enhanced neutrino-pointing accuracy. Together, these advancements are expected to significantly increase the detection of astrophysical neutrinos, paving the way for source identification and advancing the field of neutrino astronomy [47, 87].

Several telescopes currently in development, including KM3NeT in the Mediterranean Sea [48], Baikal-GVD in Lake Baikal [88], and the proposed P-ONE in the East Pacific [89], aim to complement IceCube's coverage of the TeV-PeV neutrino sky from the northern hemisphere. KM3NeT is a network of deep-sea neutrino telescopes planned for deployment in the Mediterranean Sea [48]. The KM3NeT/ARCA detector, located at the Capo Passero site in Italy, is specifically designed to detect high-energy cosmic neutrinos. KM3NeT/ARCA, with a broader field of view than IceCube, focuses on detecting Galactic sources, especially those observable at lower energies around tens of TeV. However, the observatory's sensitivity to muon neutrinos is limited [90, 91].

B. With current and future gamma-ray telescopes

Multi-messenger astrophysics has become a groundbreaking reality, propelled by recent advancements in gravitational wave, gamma-ray astronomy and high-energy neutrino detection. These breakthroughs have ushered in a new era of understanding the high-energy astrophysical universe and the mechanisms underlying its most energetic phenomena.

Over the past two decades, advancements in both space-based and ground-based gamma-ray detectors have greatly enhanced our understanding of the high-energy gamma-ray universe. At high energies (HE, $E > 0.1$ GeV), the Fermi Large Area Telescope (Fermi-LAT) continues to be a linchpin in multiwavelength and multimessenger studies [40]. Surveying the gamma-ray sky since 2008, Fermi-LAT's comprehensive energy coverage and expansive field of view have facilitated groundbreaking discoveries across eight orders of magnitude in photon energy [92]. All γ -ray data from Fermi are made publicly available in real-time, fostering collaborative research across diverse scientific communities.

Looking ahead, for Very High Energy (VHE, $E > 0.1$ TeV) observations, the next-generation ground-based gamma-ray detector, Cherenkov Telescope Array (CTA), represents a monumental leap in ground-based gamma-ray astronomy [93]. Encompassing an energy range from some tens of GeV to about 300 TeV, CTA's three arrays of Imaging Atmospheric Cherenkov telescopes promise unprecedented sensitivity and precision [94]. With a focus on extragalactic objects in the Northern Hemisphere and galactic sources in the Southern Hemisphere, CTA's vast effective area and field-of-view position it as a cornerstone instrument for future gamma-ray astronomy endeavors [94].

As the next-generation gamma-ray telescope to observe very- to ultra-high-energy gamma rays, the Southern Wide-field Gamma-ray Observatory (SWGGO), a water Cherenkov telescope array, stands at the forefront of this revolution [42]. Spanning energies from about 30 GeV to a few PeV, SWGGO provides a wide field and high-duty cycle view of the southern sky [42], complementing existing particle arrays in the Northern Hemisphere like Large High Altitude Air Shower Observatory (LHAASO) [41]. Speaking of which, LHAASO, is a multi-purpose facility designed to study cosmic rays and gamma rays across a broad energy spectrum, ranging from sub-TeV to beyond 1 PeV [95].

V. RESULTS

A. Differential flux sensitivity

Following the discussions of neutrino and gamma-ray detectors in Sec. IV, in this section, we highlight the differential flux sensitivity of these experiments towards the detection of point sources. In Fig. 1 (Left: neutrino and Right: gamma-ray experiments), we show the differential flux sensitivity of all our selected telescopes mentioned in sec. IV. For IceCube and IceCube-Gen2, we take into account the detection sensitivity (as detailed in ref. [83]) to observe the neutrino flux originating from a point source positioned at the celestial equator ($\delta = 0^0$), achieving an average significance of 5σ over a decade of observations. Here we would like to comment that the existing IceCube Observatory and the IceCube Upgrade now under construction will be fully integrated into the ultimate Gen2 facility, providing energy coverage that will range from 1 GeV to 100 PeV [46]. In this way, IceCube-Gen2 will be one of the world's preeminent atmospheric and astrophysical neutrino observatories. For KM3Net, we consider the

90% C.L. Quasi-differential sensitivity for point-like emission predicted for the full detector array [91]. The potential of the full KM3NeT is expected to discover diffuse and point-like spectra that have not been detected by IceCube yet.

Finally, for TRIDENT which is expected to be the most sensitive neutrino telescope in the upcoming days, we use the 90% C.L. median sensitivity for the point-like sources from the expected all-sky survey [47]. In this context, we want to mention that for all neutrino telescopes, we only consider their sensitivity from track-like events for the sources near declination, $\delta = 0^\circ$.

For the gamma-ray telescopes, such as CTA ([43, 44]), SWGO ([42]), LHAASO ([41, 42]) and Fermi-LAT ([39, 40]), we use the differential flux limits for point-like sources from their respective performance guidelines.

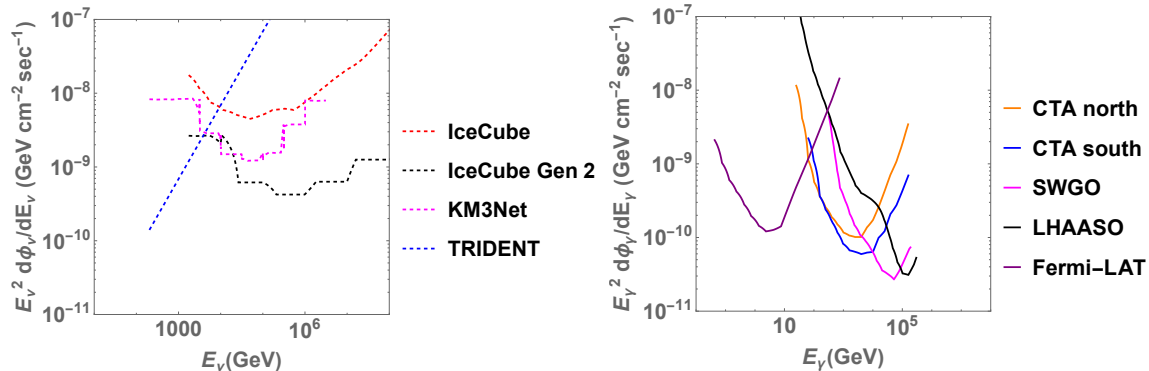


FIG. 1. Differential flux ($E_{\nu,\gamma}^2 d\phi_{\nu,\gamma}/dE_{\nu,\gamma}$) sensitivity of all our selected detectors.

B. Variation of differential flux sensitivity of neutrino telescopes with declination

In this section, we study the neutrino signals from NSs resulting from the decay of long-lived mediators produced from DM annihilation in the light of current and future-generation neutrino telescopes. This study specifically focuses on the DM-nucleon scattering cross-section in equilibrium, aiming to explore whether NSs offer a promising avenue for probing small DM-nucleon cross-sections. Throughout our investigation, we assume that DM number abundance has reached equilibrium, given the age of neutron stars considered to be larger (≥ 1 Myr) than t_{eq} . All of our selected neutrino telescopes are equally sensitive for both spin-independent (SI) and spin-dependent (SD) DM-nucleon scattering cross-sections as NSs primarily consist of neutrons.

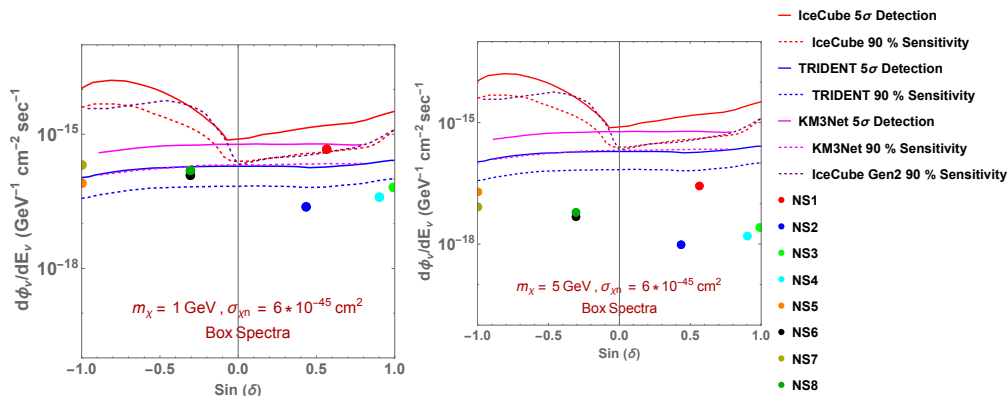


FIG. 2. Variation of flux with declination for Box-like spectra for two DM mass values.

Fig. 2 offers a comprehensive view of the 90% confidence level (C.L.) sensitivity (depicted by the dashed line) and the 5σ discovery potential (shown by the solid line), considering a source spectrum with a differential flux $\frac{dN}{dE} \propto E^{-2}$ as a function of source declination ($\sin \delta$). The ‘points’ on the graph represent individual differential muon neutrino flux

values for neutrino flux from each NS for our chosen DM mass (m_χ) and scattering cross-section ($\sigma_{\chi n}$). Neutrino flux from the sources (8 NSs from sec. II A) is obtained assuming box-like spectra resulting from the annihilation of DM through a long-lived mediator.

Fig. 2 indicates that for IceCube [45] and IceCube Gen-2[96], the highest sensitivity is concentrated around the equator, corresponding to optimal discovery potential, while it is weakest for declination values near $\sin(\delta) = \pm 1$ [45]. KM3NeT (with 6 years of projected data) [90] and TRIDENT [47], provide equal sensitivity for all the regions of the sky. This underscores the challenge of IceCube and IceCube-Gen2 of detecting events of interest amidst the background, particularly in regions where a stronger signal is required. For a source located in the southern sky, TRIDENT will have nearly 4 orders of magnitude improvement in sensitivity [47] compared to IceCube.

Consequently, given the present sensitivity of all these neutrino detectors, TRIDENT has the potential to detect the local NSs for DM mass around 1 GeV with $\sigma_{\chi n} = 6 \times 10^{-46} \text{ cm}^{-2}$. Whereas for DM mass for $m_\chi \sim 5 \text{ GeV}$, as shown in Fig. 2, the current and future telescopes are not sufficient unless brighter sources are present or DM-nucleon scattering is enhanced further. The choice of $\sigma_{\chi n} = 6 \times 10^{-46} \text{ cm}^{-2}$ is motivated by its proximity to the saturation cross-section of our designated local NSs. Once surpassing this threshold, multi-scattering becomes a factor to be taken into account.

C. Expected bounds on $\sigma_{\chi n}$ from local NSs

In this section, we aim to estimate the bounds on $\sigma_{\chi n}$ from the gamma-ray and neutrino emission resulting from DM annihilation from the local NSs within 0.6 kpc from Earth. First, we look for the emission from our selected 8 local NSs, and next, we study how the expected number of local NSs predicted from CGW boosts the current bounds.

In Fig. 3, with conservative measures, we translate the differential flux sensitivity (Fig. 1) of our selected detectors and derive the stacked constraints on $\sigma_{\chi n}$ as a function of the DM mass, m_χ by combining the flux limits from 8 local NSs (Eqs. 7 and 8). The limits shown in Fig. 3 emerge from the intricate interplay of the DM capture rate, DM density profile, and DM mass range and serve as the current constraints on $\sigma_{\chi n}$ for 8 nearby local NSs. We derive the stacked limits for box spectra (long-lived mediators) for the NFW density profile. To ensure the robustness of our findings, we validate the results against those obtained for the cored Burkert profile [97, 98]. However, our analysis reveals $\sigma_{\chi n}$ has no significant dependence on the density profile for local NSs. Consequently, this paper exclusively features results derived from the NFW halo profile.

Fig.3 highlights that with 8 local NSs, we only obtain the limits for DM mass $< 1 \text{ GeV}$, and IceCube-Gen2, IceCube, TRIDENT can provide any meaningful bounds. We do not obtain any bounds for gamma-ray detectors. Additionally, in Fig. 3, we further compare the limits with experimental bounds obtained from direct detection bounds, such as CDEX [99], PICO-60 [100], and XENON1T [101] and astrophysics limits obtained from Sun performed by IceCube DeepCore [70]. For DM mass $< 1 \text{ GeV}$, a handful of nearby NSs provide stronger bounds than obtained from XENON1T [101]. Therefore, Fig. 3 signifies that with the current limits from 8 local NSs, we only derive the bounds for DM mass $< 1 \text{ GeV}$.

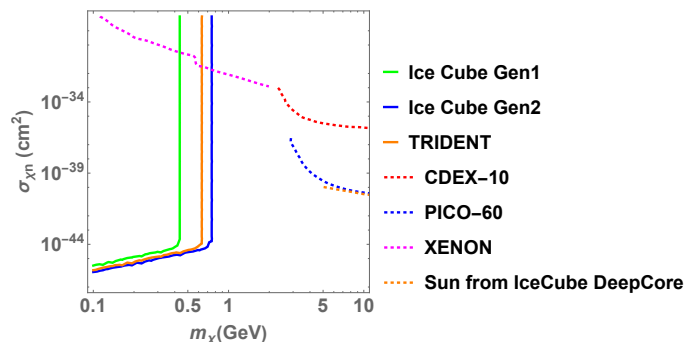


FIG. 3. Current bounds from local NSs (solid lines) and comparison with experiments (dashed lines).

We now derive the bounds on $\sigma_{\chi n}$ from the cumulative emission of the local NS population within 0.6 kpc from Earth. Following the population model proposed by ref. [38], we anticipate $N_{\text{ns}} \approx 10^5$ within 0.6 kpc from earth for NS

ellipticity $\epsilon \sim 10^{-5}$. Using the local NS population in the vicinity of Earth from CGW search, we estimate the projected bounds for gamma-ray and neutrino telescopes from the cumulative emission coming from around 600000 NSs.

In Fig. 4, we show the DM annihilation spectra (for both gamma-ray and neutrino) through long-lived mediators for energy ranging between $0.01 - 10^8$ GeV for three scattering cross-section ($\sigma_{\chi n}$) values. As mentioned before, here we consider the expected number of local NSs $N_{\text{NS}} \approx 10^5$, probed by CGW within 0.6 kpc surrounding Earth. The DM-nucleon scattering cross-section, $\sigma_{\chi n} = 10^{-46}$ cm², which is very close to the saturation cross-section limits, produces the weakest flux. The fluxes get stronger with increasing the $\sigma_{\chi n}$ values, which also motivates the multiple scatterings, and they can be probed with our selected detectors both for gamma-ray and neutrino.

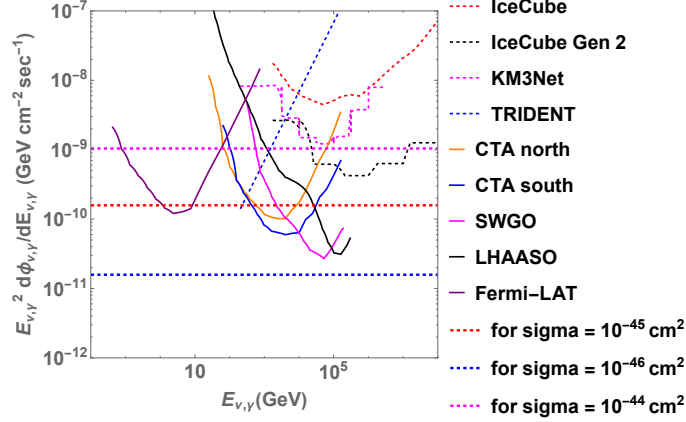


FIG. 4. DM annihilation spectra through long-lived mediators for three scattering cross-section values.

In Fig. 5, we show the projected bounds for the local NS population for box-like spectra. This figure additionally signifies that we can expect the strongest bounds from TRIDENT (for neutrino) for DM mass $< 10^3$ GeV and SWGO (for gamma-ray) for DM mass $> 10^3$ GeV. Respective bounds on $\sigma_{\chi n}$ for larger DM mass ($10^3 - 10^5$ GeV), resulting from the analysis on CTA, IceCube-Gen2, LHAASO observation is stronger than the limits from IceCube results with Sun and comparable with indirect search from H.E.S.S. based on galactic NS population.

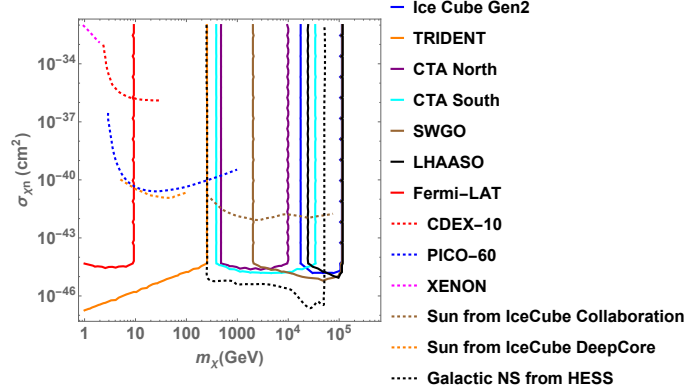


FIG. 5. Comprehensive limits on $\sigma_{\chi n}$ from local NS population with CGW searches (solid lines) and comparison with other DM direct and indirect bounds (dashed lines). See text for details.

In Fig. 5, we extend our analysis to compare our findings with the results obtained from astrophysical studies and direct detection experiments. Particularly noteworthy is the comparison with the direct detection limits established by CDEX [99], PICO-60 [100], and XENON1T [101] regarding DM-nucleon SD scattering cross-section. This comparison underscores the advantage of constraints derived from local NSs, which extend to DM masses $\sim 10^5$ GeV.

VI. DISCUSSION AND CONCLUSION

Studying DM capture by NSs could offer valuable insights into the nature of this elusive substance, shedding light on its properties and interactions with ordinary matter. This research holds promise for advancing our understanding of fundamental physics and unlocking the mysteries of the cosmos. Our motivation for this work is to target the nearby local NSs and study the DM capture rate inside them. Generally, NSs are considered to be very efficient in capturing DM with feeble interactions because of their small radius and strong lower gravitational focus power. But, to this date, only a handful number of NSs have been detected (even though they are very abundant in the galaxy $\approx 10^8$) and most of them are not very close to Earth (as compared to BDs). This eventually also weakens the bounds on scattering cross-section ($\sigma_{\chi n}$) when our goal is to detect the gamma rays and neutrinos resulting from DM annihilation with space or ground-based detectors. Recently, gravitational wave searches have gained a lot of attention which embarks our interest in the detection of local NSs being the natural source of continuous gravitational wave emission. The search of CGW indicates a substantially rich NS population adjacent to Earth and strengthens the bound on $\sigma_{\chi n}$. For the purpose of this paper, we combine the sensitivity from current and future generation gamma-ray and neutrino detectors which enables us to construct a comprehensive picture of DM signature from local NSs.

The conclusion of this article is as follows:

- Our investigation delves into the extensive analysis of the sensitivity at the 90% C.L. and the potential for 5σ discovery across present and future-generation neutrino telescopes. We specifically examine their capability to detect neutrino signals originating from our selected NSs resulting from the decay of long-lived mediators produced through DM annihilation (see Fig. 2). Among the current neutrino detectors, only TRIDENT exhibits the potential to detect neutrinos for DM masses around 1 GeV with a scattering cross-section ($\sigma_{\chi n}$) of 6×10^{-46} cm^{-2} . However, for DM masses $m_\chi \geq 5$ GeV, none of the existing neutrino telescopes are adequate unless there are brighter sources or a further enhancement in DM-nucleon scattering.
- We interpret the differential flux sensitivity (Fig.1) of our selected gamma-ray and neutrino detectors (see sec.V A) and establish stacked constraints on $\sigma_{\chi n}$ concerning m_χ by combining the flux limits from 8 nearby NSs (Fig.3) assuming an NFW density profile. Fig.3 indicates that constraints are only obtainable for DM masses < 1 GeV with 8 local NSs, and meaningful bounds can be provided by IceCube-Gen2, IceCube, and TRIDENT. No bounds are obtained for gamma-ray detectors.
- With the inclusion of a few nearby NSs (0.6 kpc), we determine that no limits can be obtained for DM masses above 1 GeV (Fig. 3). We further explore the potential impact of the expected population of local NSs from CGW searches on our current limits (Fig. 4). We follow a recent study by Reed et al. [38] which extensively surveyed CGWs originating from unidentified Galactic neutron stars near Earth to establish the number of NSs being surveyed by a given CGW investigation.
- We derive the bounds on $\sigma_{\chi n}$ from the cumulative emission of the local NS population within 0.6 kpc from Earth (Fig. 5). The cumulative emission expected from approximately 6×10^5 NSs indicates that the most stringent bounds would originate from TRIDENT (for neutrinos) for DM masses $m_\chi < 1000$ GeV and from SWGO (for gamma-rays) for DM masses $m_\chi > 1000$ GeV.
- Figs. 3 and 5, where we compare our obtained limits with experimental bounds from direct detection and astrophysical limits, further demonstrate that our results, even with only 8 nearby NSs, are competitive with existing direct detection limits and some astrophysical bounds.

The study reveals that present and upcoming neutrino and gamma-ray observatories are not very sensitive to DM-nucleon scattering when a few known local NSs within 0.6 kpc in the neighborhood of Earth are considered and can only provide a weak bound for DM mass ~ 1 GeV. Improved limits on DM-nucleon scattering cross-section can be achieved with the consideration of about 10^5 local NS population anticipated from the CGW search for a range between low (\sim sub-GeV) to heavy (\sim PeV) DM mass. The corresponding limit on $\sigma_{\chi n}$ with the local NS population is found to be on par with those obtained from DM direct search and indirect search bounds from other astrophysical sources like the Sun or Galactic NS population. Future CGW searches with better sensitivity are expected to further limit the local NS population, which can further constrain the DM-nucleon scattering with better precision.

ACKNOWLEDGMENTS

A.D.B. acknowledges financial support from DST, India, under grant number IFA20-PH250 (INSPIRE Faculty Award). Some part of P.B.'s work was supported by the EOSC Future project which was co-funded by the European Union

Horizon Programme call INFRAEOSC-03-2020, Grant Agreement 101017536. The authors would like to thank Dr. Tarak Maity and Dr. Nicholas L. Rodd for their valuable suggestions.

-
- [1] N. Aghanim *et al.* (Planck), *Astron. Astrophys.* **641**, A6 (2020), [Erratum: *Astron. Astrophys.* 652, C4 (2021)], arXiv:1807.06209 [astro-ph.CO].
- [2] T. R. Slatyer, in *Theoretical Advanced Study Institute in Elementary Particle Physics: Anticipating the Next Discoveries in Particle Physics* (2018) pp. 297–353, arXiv:1710.05137 [hep-ph].
- [3] J. M. Gaskins, *Contemp. Phys.* **57**, 496 (2016), arXiv:1604.00014 [astro-ph.HE].
- [4] A. de Lavallaz and M. Fairbairn, *Phys. Rev. D* **81**, 123521 (2010), arXiv:1004.0629 [astro-ph.GA].
- [5] J. Bramante, A. Delgado, and A. Martin, *Phys. Rev.* **D96**, 063002 (2017), arXiv:1703.04043 [hep-ph].
- [6] T. Nakajima, B. R. Oppenheimer, S. R. Kulkarni, D. A. Golimowski, K. Matthews, and S. T. Durrance, *Nature* **378**, 463 (1995).
- [7] A. Burrows, W. B. Hubbard, J. I. Lunine, and J. Liebert, *Rev. Mod. Phys.* **73**, 719 (2001), arXiv:astro-ph/0103383.
- [8] R. K. Leane, T. Linden, P. Mukhopadhyay, and N. Toro, *Phys. Rev. D* **103**, 075030 (2021), arXiv:2101.12213 [astro-ph.HE].
- [9] N. F. Bell, G. Busoni, M. E. Ramirez-Quezada, S. Robles, and M. Virgato, *JCAP* **10**, 083 (2021), arXiv:2104.14367 [hep-ph].
- [10] B. Dasgupta, A. Gupta, and A. Ray, *JCAP* **08**, 018 (2019), arXiv:1906.04204 [hep-ph].
- [11] N. F. Bell, J. B. Dent, and I. W. Sanderson, *Phys. Rev. D* **104**, 023024 (2021), arXiv:2103.16794 [hep-ph].
- [12] N. F. Bell, M. J. Dolan, and S. Robles, *JCAP* **11**, 004 (2021), arXiv:2107.04216 [hep-ph].
- [13] G. Busoni, *Moscow Univ. Phys. Bull.* **77**, 301 (2022), arXiv:2201.00048 [hep-ph].
- [14] N. F. Bell, G. Busoni, S. Robles, and M. Virgato, *JCAP* **09**, 028 (2020), arXiv:2004.14888 [hep-ph].
- [15] W. H. Press and D. N. Spergel, *Astrophys. J.* **296**, 679 (1985).
- [16] C. Kouvaris, *Phys. Rev. D* **77**, 023006 (2008), arXiv:0708.2362 [astro-ph].
- [17] S. Okawa, M. Tanabashi, and M. Yamanaka, *Phys. Rev. D* **95**, 023006 (2017), arXiv:1607.08520 [hep-ph].
- [18] I. Z. Rothstein, T. Schwetz, and J. Zupan, *JCAP* **07**, 018 (2009), arXiv:0903.3116 [astro-ph.HE].
- [19] C. Niblaeus, A. Beniwal, and J. Edsjo, *JCAP* **11**, 011 (2019), arXiv:1903.11363 [astro-ph.HE].
- [20] G. Elor, N. L. Rodd, T. R. Slatyer, and W. Xue, *JCAP* **06**, 024 (2016), arXiv:1511.08787 [hep-ph].
- [21] R. K. Leane and J. Smirnov, *Phys. Rev. Lett.* **126**, 161101 (2021), arXiv:2010.00015 [hep-ph].
- [22] P. Bhattacharjee, F. Calore, and P. D. Serpico, *Phys. Rev. D* **107**, 043012 (2023), arXiv:2211.08067 [astro-ph.HE].
- [23] J. F. Acevedo, R. K. Leane, and L. Santos-Olmsted, (2023), arXiv:2309.10843 [hep-ph].
- [24] T. N. Maity, A. K. Saha, S. Mondal, and R. Laha, (2023), arXiv:2308.12336 [hep-ph].
- [25] D. Bose, T. N. Maity, and T. S. Ray, *JCAP* **05**, 001 (2022), arXiv:2108.12420 [hep-ph].
- [26] L. S. Miranda, S. Basegmez du Pree, K. C. Y. Ng, A. Cheek, and C. Arina, *JCAP* **08**, 006 (2023), arXiv:2211.12235 [hep-ph].
- [27] Y.-X. Chen, L. Zu, Z.-Q. Xia, Y.-L. S. Tsai, and Y.-Z. Fan, *JCAP* **08**, 036 (2023), arXiv:2302.09951 [astro-ph.HE].
- [28] P. Bhattacharjee and F. Calore, (2023), arXiv:2311.18455 [astro-ph.HE].
- [29] J. F. Acevedo, J. Bramante, Q. Liu, and N. Tyagi, (2024), arXiv:2404.10039 [hep-ph].
- [30] D. Bose and S. Sarkar, *Phys. Rev. D* **107**, 063010 (2023), arXiv:2211.16982 [astro-ph.CO].
- [31] M. Baryakhtar, J. Bramante, S. W. Li, T. Linden, and N. Raj, *Phys. Rev. Lett.* **119**, 131801 (2017), arXiv:1704.01577 [hep-ph].
- [32] B. Dasgupta, R. Laha, and A. Ray, *Phys. Rev. Lett.* **126**, 141105 (2021), arXiv:2009.01825 [astro-ph.HE].
- [33] A. Finke, S. Foffa, F. Iacovelli, M. Maggiore, and M. Mancarella, *Phys. Dark Univ.* **36**, 100994 (2022), arXiv:2108.04065 [gr-qc].
- [34] S. Caride, R. Inta, B. J. Owen, and B. Rajbhandari, *Phys. Rev. D* **100**, 064013 (2019), arXiv:1907.04946 [gr-qc].
- [35] B. P. Abbott *et al.* (LIGO Scientific, Virgo), *Phys. Rev. D* **100**, 024004 (2019), arXiv:1903.01901 [astro-ph.HE].
- [36] M. Zimmermann and E. Szedenits, *Phys. Rev. D* **20**, 351 (1979).
- [37] P. D. Lasky, *Publ. Astron. Soc. Austral.* **32**, e034 (2015), arXiv:1508.06643 [astro-ph.HE].
- [38] B. T. Reed, A. Deibel, and C. J. Horowitz, *Astrophys. J.* **921**, 89 (2021), arXiv:2104.00771 [astro-ph.HE].
- [39] “Fermi-LAT Performance,” https://www.slac.stanford.edu/exp/glast/groups/canda/lat_Performance.htm (2021).
- [40] M. Ajello *et al.*, *The Astrophysical Journal Supplement Series* **256**, 12 (2021).
- [41] (2021), arXiv:2101.03508 [astro-ph.IM].
- [42] R. Conceição (SWG0), *PoS ICRC2023*, 963 (2023), arXiv:2309.04577 [hep-ex].
- [43] “CTA Performance,” <https://www.cta-observatory.org/science/ctao-performance/1472563157332-1ef9e83d-426c>.
- [44] A. Donini, I. Burelli, O. Gueta, F. Longo, E. Pueschel, D. Tak, A. Vigliano, T. Vuillamme, O. Sergijenko, and A. Sarkar (CTA Consortium), *PoS ICRC2023*, 840 (2023), arXiv:2309.14106 [astro-ph.HE].
- [45] M. G. Aartsen *et al.* (IceCube), *Phys. Rev. Lett.* **124**, 051103 (2020), arXiv:1910.08488 [astro-ph.HE].
- [46] R. Abbasi *et al.* (IceCube), *JINST* **16**, P08034 (2021), arXiv:2103.16931 [hep-ex].
- [47] Z. P. Ye *et al.*, (2022), arXiv:2207.04519 [astro-ph.HE].
- [48] S. Adrian-Martinez *et al.* (KM3Net), *J. Phys. G* **43**, 084001 (2016), arXiv:1601.07459 [astro-ph.IM].

- [49] A. Vahdat, B. Posselt, A. Santangelo, and G. G. Pavlov, *Astron. Astrophys.* **658**, A95 (2022), arXiv:2111.04791 [astro-ph.HE].
- [50] “ATNF Catalog,” https://cral-perso.univ-lyon1.fr/labo/fc/cdroms/cdrom2013/Temps/horloge_pulsar/catalogue_ATNF.xls.
- [51] R. Diehl *et al.*, *Nature* **439**, 45 (2006), arXiv:astro-ph/0601015.
- [52] R. N. Manchester, G. B. Hobbs, A. Teoh, and M. Hobbs, *Astronom. J.* **129**, 1993 (2005), arXiv:astro-ph/0412641 [astro-ph].
- [53] J. F. Navarro, C. S. Frenk, and S. D. M. White, *Astrophys. J.* **462**, 563 (1996), arXiv:astro-ph/9508025.
- [54] F. Calore, M. Cirelli, L. Derome, Y. Genolini, D. Maurin, P. Salati, and P. D. Serpico, *SciPost Phys.* **12**, 163 (2022), arXiv:2202.03076 [hep-ph].
- [55] C. Ilie, J. Pilawa, and S. Zhang, *Phys. Rev. D* **102**, 048301 (2020), arXiv:2005.05946 [astro-ph.CO].
- [56] R. Garani and S. Palomares-Ruiz, *JCAP* **05**, 042 (2022), arXiv:2104.12757 [hep-ph].
- [57] M. Pospelov, A. Ritz, and M. B. Voloshin, *Phys. Lett. B* **662**, 53 (2008), arXiv:0711.4866 [hep-ph].
- [58] M. Pospelov and A. Ritz, *Phys. Lett. B* **671**, 391 (2009), arXiv:0810.1502 [hep-ph].
- [59] B. Batell, M. Pospelov, A. Ritz, and Y. Shang, *Phys. Rev. D* **81**, 075004 (2010), arXiv:0910.1567 [hep-ph].
- [60] A. Dedes, I. Giomataris, K. Suxho, and J. D. Vergados, *Nucl. Phys. B* **826**, 148 (2010), arXiv:0907.0758 [hep-ph].
- [61] E. C. F. S. Fortes, V. Pleitez, and F. W. Stecker, *Astropart. Phys.* **74**, 87 (2016), arXiv:1503.08220 [hep-ph].
- [62] Y. Yamamoto, *EPJ Web Conf.* **168**, 06007 (2018), arXiv:1708.09756 [hep-ph].
- [63] B. Holdom, *Phys. Lett. B* **166**, 196 (1986).
- [64] B. Holdom, *Phys. Lett. B* **178**, 65 (1986).
- [65] F. Chen, J. M. Cline, and A. R. Frey, *Phys. Rev. D* **80**, 083516 (2009), arXiv:0907.4746 [hep-ph].
- [66] A. Berlin, D. Hooper, and G. Krnjaic, *Phys. Rev. D* **94**, 095019 (2016), arXiv:1609.02555 [hep-ph].
- [67] M. Cirelli, P. Panci, K. Petraki, F. Sala, and M. Taoso, *JCAP* **05**, 036 (2017), arXiv:1612.07295 [hep-ph].
- [68] M. Cirelli, Y. Gouttenoire, K. Petraki, and F. Sala, *JCAP* **02**, 014 (2019), arXiv:1811.03608 [hep-ph].
- [69] A. Ibarra, S. Lopez Gehler, and M. Pato, *JCAP* **07**, 043 (2012), arXiv:1205.0007 [hep-ph].
- [70] R. Abbasi *et al.* (IceCube), *Phys. Rev. D* **105**, 062004 (2022), arXiv:2111.09970 [astro-ph.HE].
- [71] E. Waxman and J. N. Bahcall, *Phys. Rev. D* **59**, 023002 (1999), arXiv:hep-ph/9807282.
- [72] M. G. Aartsen *et al.* (IceCube), *Science* **342**, 1242856 (2013), arXiv:1311.5238 [astro-ph.HE].
- [73] M. G. Aartsen *et al.* (IceCube), *Science* **361**, 147 (2018), arXiv:1807.08794 [astro-ph.HE].
- [74] M. G. Aartsen *et al.* (IceCube, Fermi-LAT, MAGIC, AGILE, ASAS-SN, HAWC, H.E.S.S., INTEGRAL, Kanata, Kiso, Kapteyn, Liverpool Telescope, Subaru, Swift NuSTAR, VERITAS, VLA/17B-403), *Science* **361**, eaat1378 (2018), arXiv:1807.08816 [astro-ph.HE].
- [75] R. Abbasi *et al.* (IceCube, Fermi Gamma-ray Burst Monitor), *Astrophys. J.* **939**, 116 (2022), arXiv:2205.11410 [astro-ph.HE].
- [76] M. G. Aartsen *et al.* (IceCube), *Astrophys. J.* **857**, 117 (2018), arXiv:1712.06277 [astro-ph.HE].
- [77] M. G. Aartsen *et al.* (IceCube), *Astrophys. J.* **890**, 111 (2020), arXiv:1908.09997 [astro-ph.HE].
- [78] R. Abbasi *et al.* (IceCube), *Phys. Rev. D* **106**, 022005 (2022), arXiv:2111.10169 [astro-ph.HE].
- [79] M. G. Aartsen *et al.* (IceCube), *Astrophys. J.* **835**, 45 (2017), arXiv:1611.03874 [astro-ph.HE].
- [80] K. Murase, D. Guetta, and M. Ahlers, *Phys. Rev. Lett.* **116**, 071101 (2016), arXiv:1509.00805 [astro-ph.HE].
- [81] A. Ambrosone, M. Chianese, D. F. G. Fiorillo, A. Marinelli, G. Miele, and O. Pisanti, *J. Phys. Conf. Ser.* **2156**, 012082 (2021).
- [82] K. Fang, K. Kotera, M. C. Miller, K. Murase, and F. Oikonomou, *JCAP* **12**, 017 (2016), arXiv:1609.08027 [astro-ph.HE].
- [83] M. G. Aartsen *et al.* (IceCube), (2019), arXiv:1911.02561 [astro-ph.HE].
- [84] R. Abbasi *et al.* (IceCube-Gen2), *PoS ICRC2023*, 994 (2023), arXiv:2308.09427 [astro-ph.HE].
- [85] A. Ishihara (IceCube), *PoS ICRC2019*, 1031 (2021), arXiv:1908.09441 [astro-ph.HE].
- [86] F. Hu, Z. Li, and D. Xu, *PoS ICRC2021*, 1043 (2021), arXiv:2108.05515 [astro-ph.IM].
- [87] M. G. Aartsen *et al.* (IceCube), *Nature* **551**, 596 (2017), arXiv:1711.08119 [hep-ex].
- [88] A. Avrorin *et al.*, *Nucl. Instrum. Meth. A* **639**, 30 (2011).
- [89] M. Agostini *et al.* (P-ONE), *Nature Astron.* **4**, 913 (2020), arXiv:2005.09493 [astro-ph.HE].
- [90] S. Aiello *et al.* (KM3NeT), *Astropart. Phys.* **111**, 100 (2019), arXiv:1810.08499 [astro-ph.HE].
- [91] in *38th International Cosmic Ray Conference* (2023) arXiv:2309.05016 [astro-ph.HE].
- [92] W. B. Atwood and and, *The Astrophysical Journal* **697**, 1071 (2009).
- [93] R. Zanin *et al.* (CTA Observatory, CTA Consortium, LST), *PoS ICRC2021*, 005 (2022).
- [94] O. Gueta (CTA Consortium, CTA Observatory), *PoS ICRC2021*, 885 (2021), arXiv:2108.04512 [astro-ph.IM].
- [95] Z. Cao (LHAASO), *Chin. Phys. C* **34**, 249 (2010).
- [96] A. Omeliukh *et al.* (IceCube-Gen2), *PoS ICRC2021*, 1184 (2021), arXiv:2107.08527 [astro-ph.HE].
- [97] A. Burkert, *Astrophys. J. Lett.* **447**, L25 (1995), arXiv:astro-ph/9504041.
- [98] P. Salucci and A. Burkert, *Astrophys. J. Lett.* **537**, L9 (2000), arXiv:astro-ph/0004397.
- [99] H. Jiang *et al.* (CDEX), *Phys. Rev. Lett.* **120**, 241301 (2018), arXiv:1802.09016 [hep-ex].
- [100] C. Amole *et al.* (PICO), *Phys. Rev. D* **100**, 022001 (2019), arXiv:1902.04031 [astro-ph.CO].
- [101] E. Aprile *et al.* (XENON), *Phys. Rev. Lett.* **123**, 241803 (2019), arXiv:1907.12771 [hep-ex].